Supporting Information

The following Supporting Information is available for this article:

S1 Table. Algorithms of post-translational modifications for ABCA4 (p.A1794D and p.P1948L) and RDH11 p.E79K exchanges**.**

Algorithm	Description	Reference	Site
NetworKIN	Prediction of in vivo kinase-substrate relationships	Linding R, Jensen LJ, Ostheimer GJ, *et al*. Systematic discovery of in vivo phosphorylation networks. *Cell*. 2007;129:1415-1426	http://networkin.info/
NetPhorest	Non-redundant collection of 222 sequence-based classifiers for linear motifs in phosphorylation-dependent signaling	Miller ML, Jensen LJ, Diella F, *et al*. Linear Motif Atlas for Phosphorylation-Dependent Signaling. *Sci Signal*. 2008;1:ra2	http://netphorest.info/
NetPhos 3.1 Server	Prediction of serine, threonine or tyrosine phosphorylation sites	Blom N, Gammeltoft S, Brunak S. Sequence- and structure-based prediction of eukaryotic protein phosphorylation sites. *J Mol Biol*. 1999;294:1351-1362.	http://www.cbs.dtu.dk/services/NetPhos/
iSNO-PseAAC	Prediction of cysteine S-nitrosylation sites in proteins	Yan Xu, Jun Ding, Ling-Yun Wu, Kuo-Chen Chou. iSNO-PseAAC: Predict cysteine S-nitrosylation sites in proteins by incorporating position specific amino acid propensity into pseudo amino acid composition. *PLoS One*. 2013;8:e55844	http://app.aporc.org/iSNO-PseAAC/index.html
iSNO-AAPair	Prediction of cysteine S-nitrosylation sites in proteins	Chou KC. "Some remarks on protein attribute prediction and pseudo amino acid composition (50th Anniversary Year Review). *J Theor Biol*. 2011;273:236-247	http://app.aporc.org/iSNO-AAPair/
PredHydroxy	Prediction of Protein Hydroxylation Site	Shi SP, Chen X, Xu HD, Qiu JD. PredHydroxy: computational prediction of protein hydroxylation site locations based on the primary structure. *Mol Biosyst*. 2015;11:819-825	http://bioinfo.ncu.edu.cn/PredHydroxy.aspx
pSumo-CD	Prediction of sumoylation sites in proteins	Jia J, Zhang L, Liu Z, Xiao X, Chou KC. pSumo-CD: predicting sumoylation sites in proteins with covariance discriminant algorithm by incorporating sequence-coupled effects into general PseAAC. *Bioinformatics*.	http://www.jci-bioinfo.cn/pSumo-CD

		2016;32:3133-3141	
iCar-PseCp	Prediction of carbonylation sites in proteins	Jia J, Liu Z, Xiao X, Liu B, *et al*. iCar-PseCp: identify carbonylation sites in proteins by Monte Carlo sampling and incorporating sequence coupled effects into general PseAAC. *Oncotarget*. 2016;7:34558-34570	http://www.jci-bioinfo.cn/iCar-PseCp
Ptpset	Prediction of dephosphorylation site	n/a	http://bioinfo.bjmu.edu.cn/ptpset/
ESA-UbiSite	Prediction of human ubiquitination sites	Wang JR, Huang WL, Tsai MJ, Hsu KT, *et al*. ESA-UbiSite: accurate prediction of human ubiquitination sites by identifying a set of effective negatives. *Bioinformatics*. 2017;33:661-668	http://iclab.life.nctu.edu.tw/iclab_webtools/ESAUbiSite/
NGlyc	Prediction of N-Glycosylation sites in human proteins	Gupta R, Jung E, Brunak S. Prediction of N-glycosylation sites in human proteins. In preparation, 2004	http://www.cbs.dtu.dk/services/NetNGlyc/
Myristoylator	Prediction of myristoylation sites	n/a	http://mendel.imp.ac.at/myristate/SUPLpredictor.htm
Phogly-PseAAC	Prediction of lysine phosphoglycerylation in proteins	Xu Y, Ding YX, Ding J, Deng NY. Phogly-PseAAC: prediction of lysine phosphoglycerylation in proteins incorporating with position-specific propensity. *J Theor Biol*. 2015;379:10-15	http://app.aporc.org/Phogly-PseAAC/
N-Ace	Prediction of protein acetylation site	n/a	http://n-ace.mbc.nctu.edu.tw/
MDD-SOH	Prediction of S-sulfenylation sites	Bui VM, Lu CT, Ho TT, Lee TY. MDD-SOH: exploiting maximal dependence decomposition to identify S-sulfenylation sites with substrate motifs. *Bioinformatics*. 2016;32:165-712	http://csb.cse.yzu.edu.tw/MDDSOH/
GPI-SOM	Prediction of GPI-anchor signals	Fankhauser N, Maeser P. Identification of GPI-anchor signals by a Kohonen Self Organizing Map. *Bioinformatics*. 2005;21:1846-1852	http://gpi.unibe.ch/
ModPred	Predicton of potential post-translational modification sites	Pejaver V, Hsu WL., Xin F, Dunker AK., *et al*. The structural and functional signatures of proteins that undergo multiple events of post-translational modification. *Protein Sci*. 2014;23:1077-1093	http://www.modpred.org/
iNitro-Tyr	Prediction of nitrotyrosine sites in proteins	Xu Y, Wen X, Wen LS, Wu LY, *et al*. iNitro-Tyr: Prediction of nitrotyrosine sites in proteins with general pseudo amino acid composition. *PLoS One*. 2014;9:e105018	http://app.aporc.org/iNitro-Tyr/

n/a, not available data.

S2 Table. Variants in the *ABCA4* gene of patients F1:IV.13 and F1:IV.17.

Position (hg19)	Exon	dbSNP ID	Variant (NM_000350.2)	Amino-acid change	Genotype	Function	MAF (Ion Reporter)
chr1:94578548	2	rs4847281	c.141A>G	p.(=)	*C/C*	Synonymous	AMAF=0.0361:EMAF=1.0E-4:GMAF=0.0123
chr1:94549083	intronic	rs574741	c.769-86A>G	none	*C/C*	.	n/a
chr1:94549029	intronic	rs526016	c.769-32T>C	none	*A/G*	.	AMAF=0.1231:EMAF=0.3071:GMAF=0.2449
chr1:94544276	10	rs4147830	c.1240-14C>T	none	*G/A*	.	AMAF=0.4762:EMAF=0.46:GMAF=0.4655
chr1:94544234	10	rs3112831	c.1268A>G	p.H423R	*T/C*	Missense	AMAF=0.1655:EMAF=0.3094:GMAF=0.2606
chr1:94495930	intronic	rs547806	c.4352+54A>G	none	*C/C*	.	n/a
chr1:94487354	intronic	rs472908	c.4773+48C>T	none	*G/A*	.	AMAF=0.2502:EMAF=0.4309:GMAF=0.3698
chr1:94480178	38	rs61751406	c.5381C>A	p.A1794D	*G/T*	Missense	n/a
chr1:94476388	40	rs1801574	c.5682G>C	p.(=)	*C/G*	Synonymous	AMAF=0.2444:EMAF=0.2517:GMAF=0.2493
chr1:94474452	Intronic	rs4147856	c.5715-25A>C	none	*T/G*	.	AMAF=0.2376:EMAF=0.1913:GMAF=0.207
chr1:94474328	41	rs4147857	c.5814A>G	p.(=)	*T/C*	Synonymous	AMAF=0.2376:EMAF=0.1912:GMAF=0.2069
chr1:94473896	Intronic	rs2275031	c.5836-43C>A	none	*G/T*	.	AMAF=0.2329:EMAF=0.1849:GMAF=0.2011
chr1:94473864	Intronic	rs1800739	c.5836-11G>A	none	*C/T*	.	AMAF=0.2549:EMAF=0.1845:GMAF=0.2084
chr1:94473845	42	rs56142141:rs2275029	c.5843_5844delCAinsTG	p.P1948L	*TG/CA*	Missense	AMAF=0.2345:EMAF=0.1819:GMAF=0.1997
chr1:94471154	Intronic	rs4147863	c.6006-16G>A	none	*C/T*	.	AMAF=0.1552:EMAF=0.1829:GMAF=0.1735
chr1:94471075	44	rs1762114	c.6069T>C	p.(=)	*G/G*	Synonymous	AMAF=0.4682:EMAF=0.0667:GMAF=0.2243

AMAF, African American minor allele frequency.
EMAF, European American minor allele frequency.
GMAF, Global minor allele frequency.
n/a, not available data.

S3 Table. Candidate variants on the ABraOM database.

Gene	dbSNP ID	Allele count	Allele number	Homozygotes	Frequency
ABCA4	*rs61751406*	Not found	Not found	Not found	Not found
ABCA4	rs56142141	45	1218	0	0.036946
ABCA4	rs547806	1205	1218	596	0.989327
RDH11	rs80140987	30	1218	1	0.024631
CERKL	rs121909398	1	1218	0	0.000821
TLR4	chr9:120476307	Not found	Not found	Not found	Not found
CRX	rs61748438	3	1218	0	0.002463
GUCA1B	rs137853903	7	1218	0	0.005747
TLR3	rs353113432	2	1218	0	0.001642

S4 Table. Prioritized variants by The Exomiser.

Patient ID	Gene	dbSNP ID	Exomiser Score	Phenotype Score	Variant Score	Random walk similarity score
F1:IV.13	*ABCA4*	rs61751406/rs56142141	1	0.725	0.864	0.725
	CRX	rs61748438	1	0.353	0.704	0.707
	TLR3	rs35311343	1	0.704	0.831	0.704
F1:IV.17	*TLR4*	Novel	1	0.704	0.862	0.704
	ABCA4	rs61751406/rs56142141	1	0.725	0.864	0.725
	TLR4	Novel	1	0.704	0.862	0.704

S5 Table. Results of Swiss-Model modelling of RDH11 templates.

Name	Title	Residue at position 79	Identity of normal sequence target	Identity of E79K target sequence	Method	Oligo State	Ligants
3tzq.1.A	Short-chain type dehydrogenase/reductase	T	23.51	23.51	X-ray, 2.5Å	homo-tetramer	None
3r1i.1.A	Short-chain type dehydrogenase/reductase	V	24.89	24.79	X-ray, 2.0Å	homo-tetramer	4 x MG
3pk0.1.A	Short-chain type dehydrogenase/reductase SDR	A	24.05	23.95	X-ray, 1.9Å	homo-tetramer	6 x CA
4nbw.1.B	Short-chain type dehydrogenase/reductase SDR	E	27.90	27.78	X-ray, 2.0Å	homo-tetramer	4 x NAD
4nbw.1.A	Short-chain type dehydrogenase/reductase SDR	E	27.90	27.78	X-ray, 2.0Å	homo-tetramer	4 x NAD
2qq5.1.A	Dehydrogenase/reductase SDR family member 1	E	26.69	26.69	X-ray, 1.8Å	Homo-dimer	None
4fn4.1.A	Short chain dehydrogenase	F	-	26.07	X-ray, 1.8Å	homo-tetramer	4 x NAD
3tox.1.A	Short chain dehydrogenase	A	22.82	22.82	X-ray, 1.9Å	homo-tetramer	4 x NAD

S6 Table. RDH11 protein prediction of PTMs–lysine phosphoglycerylation by Phogly PseAAC.

Predicted hydrolysine site position	Peptides	Positve Score	Negative Score
55	GANTGIG**K**ETAKELA	4.505	5.025
77	LACRDVE**K**GKLVAKE	3.152	3.972
79	CRDVEKG**K**LVAKEIQ	5.586	5.618
119	KGFLAEE**K**HLHVLIN	4.916	4.991
163	LTHLLLE**K**LKESAPS	2.88	3.156
194	FHNLQGE**K**FYNAGLA	4.391	4.506

S7 Table. RDH11 protein prediction of PTMs by Modpred.

Residue	Modification	Sequence	Score	Confidence
E79	ADP-ribosylation	RVYLACRDVEKG**E**LVAKEIQTTTGN	0.17	Not modified
E79	Amidation	RVYLACRDVEKG**E**LVAKEIQTTTGN	0.40	Not modified
E79	Carboxylation	RVYLACRDVEKG**E**LVAKEIQTTTGN	0.27	Not modified
E79	Proteolytic_cleavage	RVYLACRDVEKG**E**LVAKEIQTTTGN	0.48	Not modified
K79	Acetylation	RVYLACRDVEKG**K**LVAKEIQTTTGN	0.50	Low
K79	Amidation	RVYLACRDVEKG**K**LVAKEIQTTTGN	0.27	Not modified
K79	Hydroxylation	RVYLACRDVEKG**K**LVAKEIQTTTGN	0.00	Not modified
K79	Methylation	RVYLACRDVEKG**K**LVAKEIQTTTGN	0.35	Not modified
K79	Proteolytic cleavage	RVYLACRDVEKG**K**LVAKEIQTTTGN	0.55	Low
K79	PUPylation	RVYLACRDVEKG**K**LVAKEIQTTTGN	0.17	Not modified
K79	SUMOylation	RVYLACRDVEKG**K**LVAKEIQTTTGN	0.17	Not modified
K79	Ubiquitination	RVYLACRDVEKG**K**LVAKEIQTTTGN	0.29	Not modified

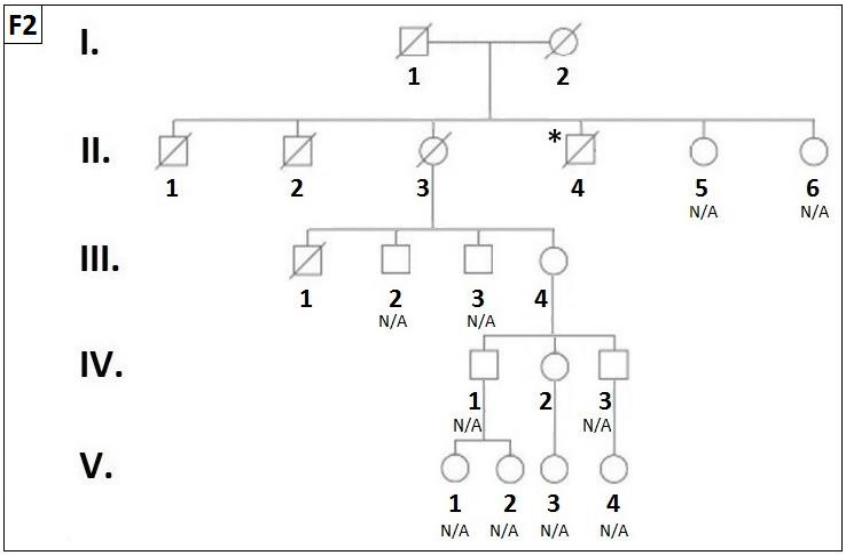

S1 Fig. Pedigree of the father's family of the siblings (F2). No candidate variant was found. N/A: DNA sample not available.

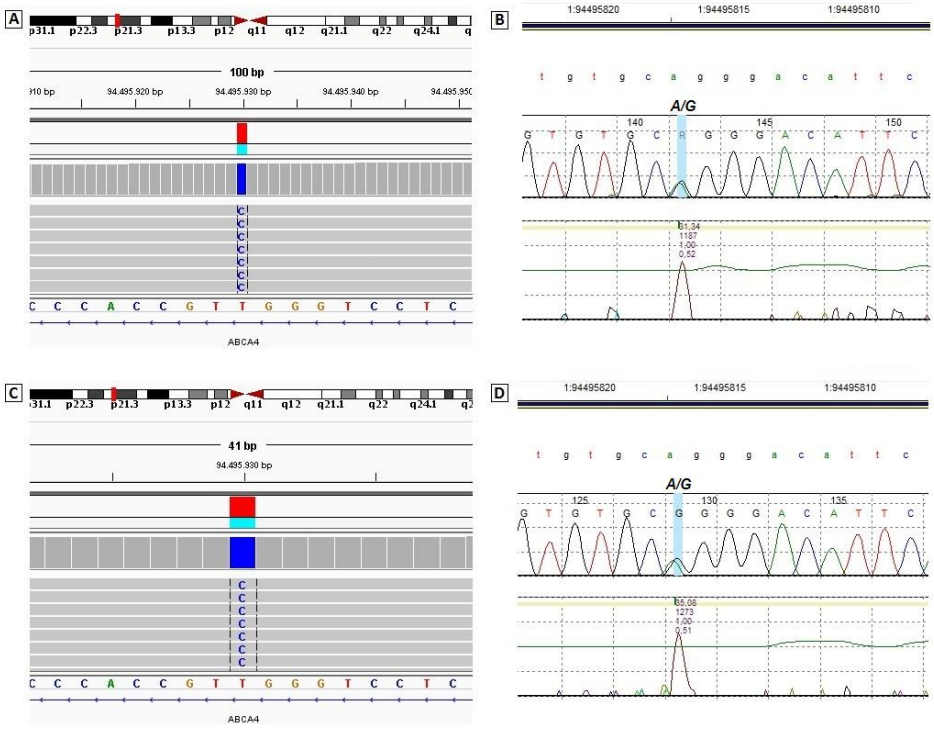

S2 Fig. DNA sequence results by WES and Sanger sequencing of *ABCA4*rs547806:A>G*.

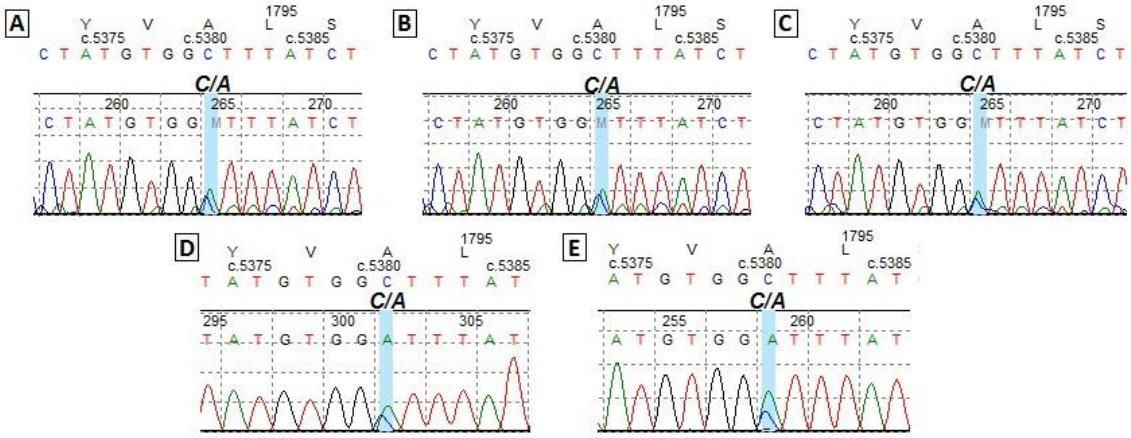

S3 Fig. Family members electropherograms of *ABCA4*rs61751406:C>A*.

S4 Fig. DNA sequence electropherograms of *ABCA4*rs56142141:C>T* and *ABCA4*rs2275029:A>G*.

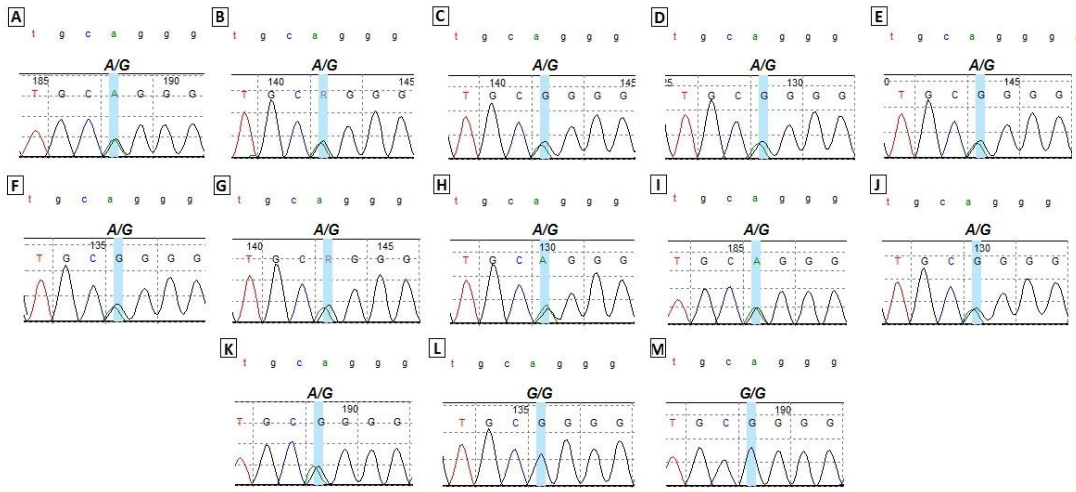

S5 Fig. DNA sequence electropherograms of *ABCA4*rs547806:A>G*.

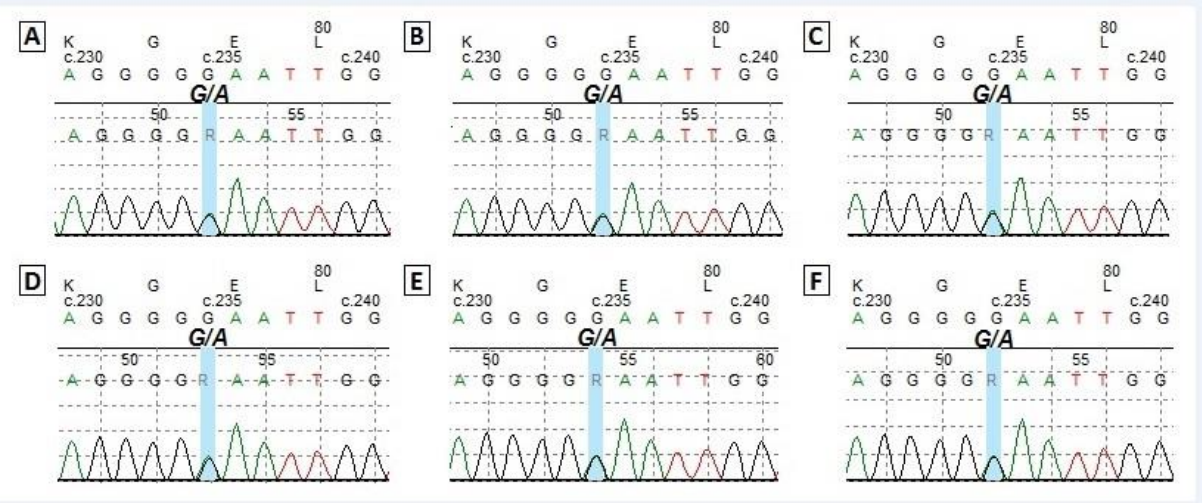

S6 Fig. DNA sequence electropherograms of *RDH11*rs80140987:G>A*.

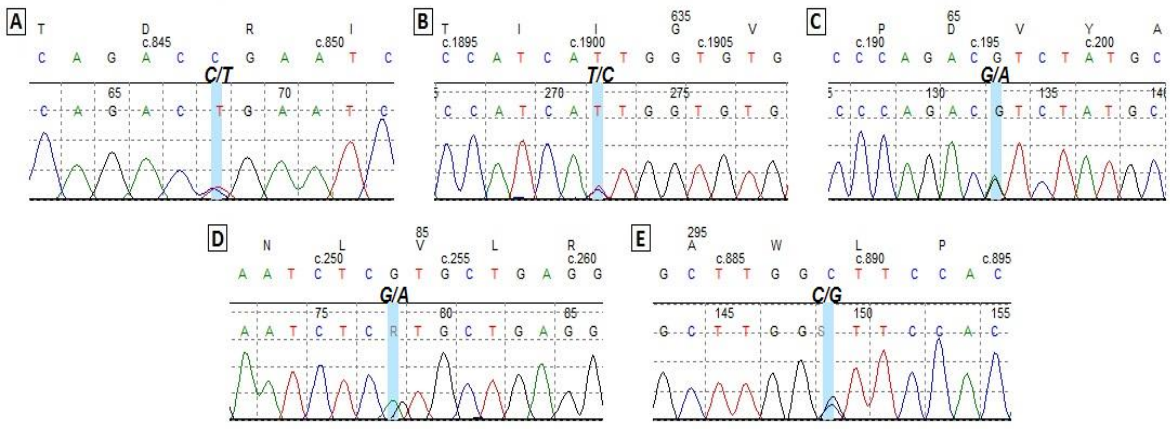

S7 Fig. DNA sequence electropherograms of variants in retinal dystrophy-related genes of patient F1:IV.13.

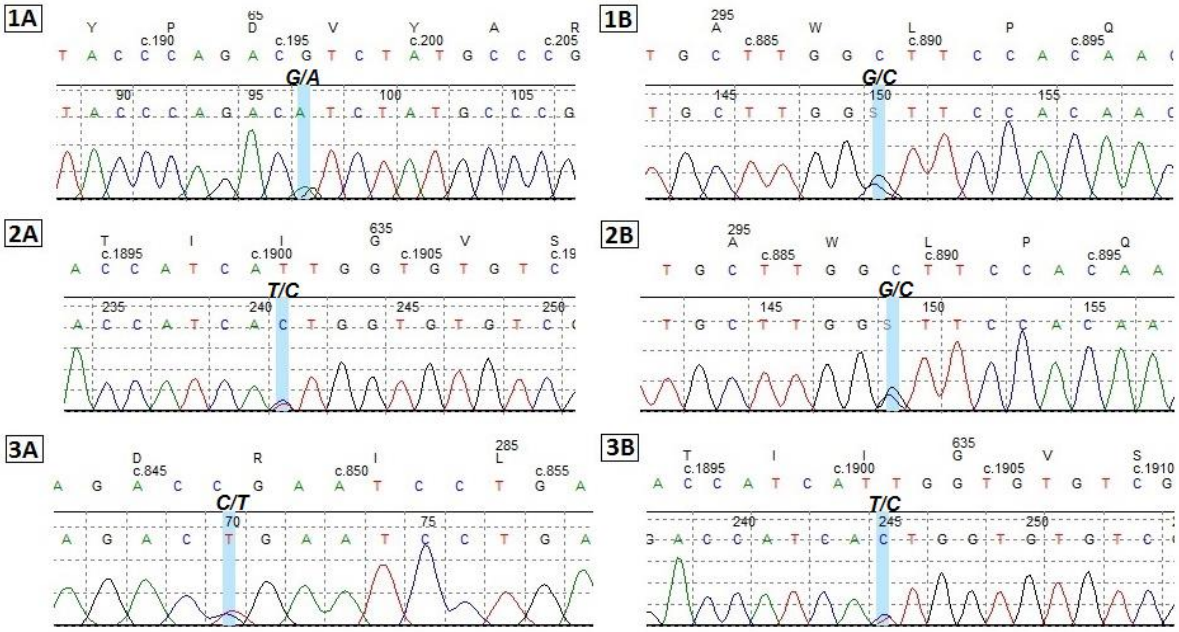

S8 Fig. DNA sequence electropherograms of variants in retinal dystrophy-related genes.

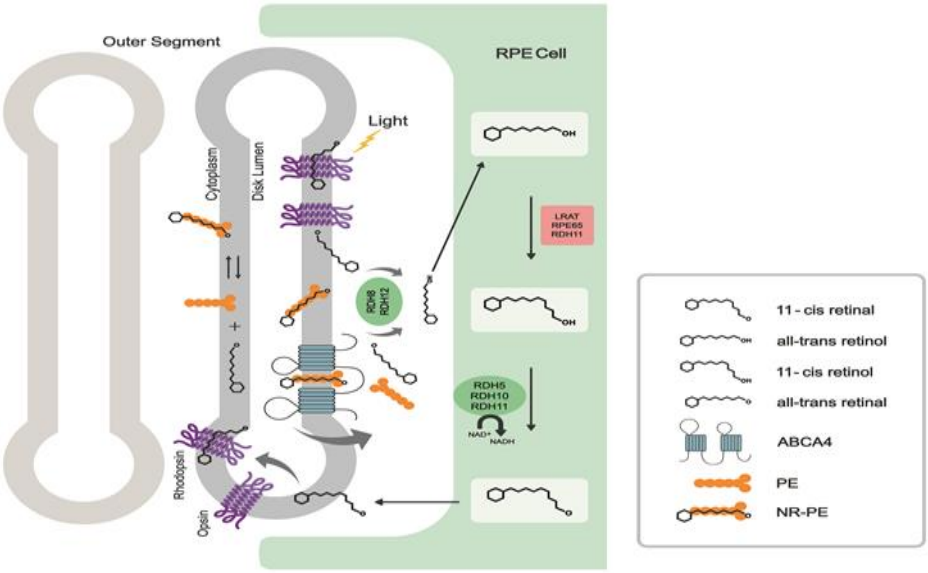

S9 Fig. The retinoid cycle enzymatic reactions.

The visual cycle begins with the absorption of light by visual pigments, called rhodopsin, present in the outer segment (OS) disk membranes of photoreceptor cells and proceeds with several enzymatic reactions aiming to recycle the light-sensitive chromophore 11-*cis* retinal to be re-stimulated by a next photon. In the dark, the 11-*cis* retinal is covalently

attached to opsin and light stimulation results in its isomerization to all-*trans* retinal, which diffuses across membrane to the cytoplasmic side. Then it is enzymatically reduced to all-*trans* retinol and transported to the RPE, where it is converted to 11-*cis* retinol and oxidized to 11-*cis* retinal, which is returned to the OS disks for the regeneration of photosensitive rhodopsin. Alternatively, a fraction of all-*trans* retinal will react with phosphatidylethanolamine (PE) forming N-retinylidene-PE (NR-PE) being actively transported across the membrane by ABCA4 [84]. When on the cytoplasmic side, NR-PE dissociates into PE and all-*trans* retinal that is equally reduced and transported to RPE. Whenever ABCA4 activity is reduced or absent, NR-PE accumulates on the lumen side of

disk membranes and reacting with another molecule of all-*trans* retinal produces toxic retinoids. As a result, lipofuscin concentration increases in the RPE leading to photoreceptor degeneration and vision loss [84-87]. Thus, *ABCA4*rs61751406:C>A* and *RDH11*rs80140987:G>A* may impair the visual cycle twice, probably causing insufficient supply of chromophores and an excess of toxic retinoids in the RPE.